

Unscented Kalman filter for time varying spectral analysis of earthquake ground motions

Dong Yinfeng^{a,*}, Li Yingmin^a, Xiao Mingkui^a, Lai Ming^b

^a College of Civil Engineering, Chongqing University, Chongqing 400045, China

^b Department of Science and Technology, Ministry of Construction, Beijing 100835, China

Received 3 June 2007; received in revised form 10 November 2007; accepted 13 November 2007

Available online 3 December 2007

Abstract

A novel parametric time-domain method for time varying spectral analysis of earthquake ground motions is presented. Based upon time varying autoregressive moving average (ARMA) modeling of earthquake ground motion, unscented Kalman filter (UKF) is used to estimate the time varying ARMA coefficients. Then, time varying spectrum is yielded according to the time varying ARMA coefficients. Analysis of the ground motion record El Centro (1940, N–S) shows that compared to Kalman filter (KF) based method, short-time Fourier transform (STFT) and wavelet transform (WT), UKF based method can more reasonably represent the distribution of the seismic energy in time–frequency plane, which ensures its better ability to track the local properties of earthquake ground motions and to identify the systems with nonlinearity. Analysis of the seismic response of a building during the 1994 Northridge earthquake shows that UKF based method can be potentially a useful tool for structural damage detection and health monitoring. Lastly, it is found that the theoretical frequency resolving power of ARMA models usually neglected in some studies has considerable effect on time varying spectrum and it is one of the key factors for ARMA modeling of earthquake ground motion.

© 2007 Elsevier Inc. All rights reserved.

Keywords: Earthquake ground motions; Time varying spectrum; Autoregressive moving average model; Unscented Kalman filter; Kalman filter

1. Introduction

Recent research studies have indicated that the conventional properties of earthquake ground motions (e.g., the properties of amplitude, frequency and duration), are not so enough as to thoroughly influence the characteristics of structural seismic response and other properties (e.g., the nonstationary properties in amplitude and frequency contents) can also influence the structural seismic response significantly [1]. To describe these nonstationary properties efficiently, some notions have been introduced for practical purpose (e.g., the zero-crossing rate is used to describe the nonstationarity in frequency contents and the time varying spectrum is

* Corresponding author. Tel.: +86 23 6512 1991; fax: +86 23 6512 3361.

E-mail address: yvhson@cta.cq.cn (Y. Dong).

used to describe the nonstationarity both in amplitude and frequency contents). Among these notions, the time varying spectrum is thought as the most suitable one, for it can provide a proper description of energy distribution in time and frequency domains. The modeling and estimation of time varying spectrum has been an open issue for the characterization of earthquake ground motions.

In most cases, the methods for estimating time varying spectrum can be classified as nonparametric and parametric. The nonparametric methods chiefly comprise time–frequency analysis (e.g., short-time Fourier transform, spectrogram and Wigner–Ville distribution [2,3]), higher order spectral analysis, evolutionary spectrum, wavelet transform and Hilbert–Huang transform (HHT), etc., [4–8]. Though successful applications of them have been reported, additional modeling processes are needed if they are used to study the attenuation laws of time varying spectrum and to synthesize ground motions for seismic design considering the nonstationary properties. The parametric methods mainly refer to the modern spectral estimation methods based on autoregressive moving average (ARMA) models. They complement the nonparametric counterparts and offer advantages such as representation parsimony, improved accuracy, resolution, and tracking, thus they are more suitable for modeling and attenuation laws determination of time varying spectrum and selection or synthesis of ground motions for seismic design [9–11].

The parametric methods consists of four steps usually, i.e., (1) time varying ARMA modeling of earthquake ground motions, (2) state-space representations of time varying ARMA models, (3) recursive estimation of time varying coefficients (states), and (4) time varying spectrum estimation according to the time varying coefficients. The time varying coefficients estimation is the core of parametric methods and it has significant influence on precision and reliability of estimation results.

The commonly used methods for time varying coefficients estimation are Kalman filter family methods [12–16], grid based filter and particle (Monte Carlo) filter [15,17]. The Kalman filter family methods include standard Kalman filter (KF) [11–16], square root Kalman filter (SRKF) [16], extended Kalman filter (EKF) [14–16], least mean square (LMS) method, recursive least square (RLS, or so called forgetting factor) method [14,15] and Kalman (Rauch–Tung–Striebel) smoother [15,16]. They are optimal methods in the sense of least square error only when the driving noises are Gaussian and the state-space models are linear. While in cases that the noises are non-Gaussian or the models are nonlinear, the Gaussian assumption of the non-Gaussian noises and the linearization of the nonlinear models can lead to suboptimal performance and sometimes divergence of the filter. On the contrary, the grid based filter and particle filter are universal methods in the framework of Bayesian principle and they can handle non-Gaussian noises and nonlinear models cases. These two methods use a large number of random sample points drawn from a prior proposal distribution to recursively estimate the states and the corresponding covariance, thus the computational complexity of them increases drastically as the dimensionality of states increases and the estimation precision relies on the knowledge of the prior distribution of states, which has blocks their utilization in practice.

To address above problems, considerable attention has been paid to the improved Kalman filter, the unscented Kalman filter (UKF) which uses a minimal set of determinate sample points (Sigma points) to completely capture the true mean and covariance of the states via unscented transformation and has been proved to be a universal, simple and precise method [15,18–21]. Thus in this paper the UKF based method is employed to estimate the time varying coefficients of ARMA models.

2. ARMA modeling and time varying spectrum estimation

2.1. Time varying ARMA modeling of earthquake ground motion

Generally the earthquake ground motion y_k as a realization of a nonstationary random process can be formulated as following time varying ARMA (p, q) model [9–11,22–24]:

$$y_k - \phi_{1,k}y_{k-1} - \cdots - \phi_{p,k}y_{k-p} = e_k - \theta_{1,k}e_{k-1} - \cdots - \theta_{q,k}e_{k-q}, \quad (1)$$

where e_k is Gaussian noise and $e_k \sim N(0, \sigma_k^2)$. σ_k is also called envelope function. The variables $\{\phi_{i,k} i = 1, 2, \dots, p\}$ and $\{\theta_{i,k} i = 1, 2, \dots, q\}$ are the time varying autoregressive (AR) coefficients and moving average (MA) coefficients, respectively. The subscript k denotes the instant $t = k\Delta t$ where Δt is the sampling time.

Besides above method, another notable method based on functional series ARMA model is also often used for the modeling and analysis of earthquake ground motions, in which the AR and MA coefficients are represented as the weighted sum of a set of deterministic basis functions. The time varying weighting or so-called projection coefficients are the parameters to be estimated and the AR and MA coefficients are derived from weighted sum of the basis functions. The method is more complicated and the proper selection of basis functions is still an issue to be studied, thus the method will not be discussed in this paper. For more details the readers are referred to [9].

2.2. Time varying spectrum estimation

The time varying spectrum can be yielded according to the time varying ARMA coefficients as given by [9–11]

$$p(f, k) = 2\sigma_k^2 \frac{|1 - \theta_{1,k}e^{-i2\pi f\Delta t} - \dots - \theta_{q,k}e^{-i2\pi qf\Delta t}|^2}{|1 - \phi_{1,k}e^{-i2\pi f\Delta t} - \dots - \phi_{p,k}e^{-i2\pi pf\Delta t}|^2} \Delta t, \quad (2)$$

where f is frequency (Hz) and $f \in [0, f_s/2]$. f_s is the sampling frequency and $f_s = 1/\Delta t$.

2.3. Order selection of time varying ARMA models

The order selection of time varying ARMA models is an important factor to be considered for time varying spectrum estimation. As for time invariant ARMA models, the orders can be selected parsimoniously according to the well-known Akaike Information Criterion (AIC) or other criteria in the sense of minimal realization of linear systems [25–27]. But for time varying ARMA models, such criteria no longer hold true and theoretically the orders should also be time varying, which would make the order selection of time varying ARMA models an arduous task. While considering the spectral properties of a time varying ARMA model, a fixed order can be properly selected to achieve satisfactory accuracy for practical purpose. First, an optimal order can be determined based on the time invariant ARMA model using the AIC or other criteria. Then, the effective frequency ranges for ARMA models are checked. It was pointed out in [28] that for an ARMA (p, q) model its effective frequency range in distinguishing adjacent spectral peaks was $[f_s/8(p+q), f_s/2 - f_s/4(p+q)]$. Thus the selected order should assure the concerned spectral peaks locate in the effective frequency range.

3. State-space representations of time varying ARMA models

Usually a time varying ARMA (p, q) model can be represented as following state-space model [11,29]:

$$\mathbf{X}_k = \mathbf{X}_{k-1} + \mathbf{V}_{k-1}, \quad (3)$$

$$y_k = \mathbf{H}_k^T \mathbf{X}_k + e_k. \quad (4)$$

In Eq. (3), $\mathbf{X}_k = [\phi_{1,k}, \dots, \phi_{p,k}, -\theta_{1,k}, \dots, -\theta_{q,k}]^T$ is called state vector and $\mathbf{V}_k = [v_{1,k}, \dots, v_{p+q,k}]^T$ is Gaussian process noise where $\mathbf{V}_k \sim N(0, \mathbf{Q}_k)$. In Eq. (4), $\mathbf{H}_k = [y_{k-1}, \dots, y_{k-p}, e_{k-1}, \dots, e_{k-q}]^T$ is the measurement vector and e_k , which is the same as that in Eq. (1), is also called measurement noise. Eq. (3) indicates the transition of the state from one moment to the next and Eq. (4) represents the noisy observation of the inaccessible state. Moreover, the assumption that \mathbf{V}_k and e_k are mutual independent is made.

Besides above model, other two dual estimation models are also often used for representing time varying ARMA models as state-space models [29]. For these dual estimation models, the states and parameters are estimated at the same time and they are only suitable for the case of large Signal to Noise Ratio (SNR). When the SNR is small, their performance will degrade sharply. While for above model, the state consists of the time varying ARMA coefficients only and its performance is quite well even if the SNR is very small [29]. Thus, the state-space model represented by Eqs. (3) and (4) is used here to represent the time varying ARMA models.

4. Estimation of state-space model with Kalman filter and Unscented Kalman filter

4.1. Estimation of state-space model using Kalman filter

The recursive estimation of the state-space model with Kalman filter mainly consists of following steps [9–16]:

$$\hat{\mathbf{P}}_{k+1} = \mathbf{P}_k + \mathbf{Q}_{k+1}, \quad (5)$$

$$\mathbf{K}_{k+1} = \hat{\mathbf{P}}_{k+1} \mathbf{H}_{k+1}^T (\mathbf{H}_{k+1}^T \hat{\mathbf{P}}_{k+1} \mathbf{H}_{k+1} + \sigma_{k+1}^2)^{-1}, \quad (6)$$

$$\mathbf{X}_{k+1} = \mathbf{X}_k + \mathbf{K}_{k+1} (y_{k+1} - \mathbf{H}_{k+1}^T \mathbf{X}_k), \quad (7)$$

$$\mathbf{P}_{k+1} = (\mathbf{I} - \mathbf{K}_{k+1} \mathbf{H}_{k+1}^T) \hat{\mathbf{P}}_{k+1}, \quad (8)$$

where $\hat{\mathbf{P}}_{k+1}$ is the prediction covariance of state, \mathbf{P}_{k+1} is the posterior covariance of state and \mathbf{K}_{k+1} is called Kalman gain. The notation in the right hand of Eq. (7), $e_{k+1} = y_{k+1} - \mathbf{H}_{k+1}^T \mathbf{X}_k$, is called prediction error and the notation, $\hat{e}_{k+1} = y_{k+1} - \mathbf{H}_{k+1}^T \mathbf{X}_{k+1}$, calculated according to \mathbf{X}_{k+1} , is called residue.

If Eqs. (5) and (6) are rewritten as

$$\hat{\mathbf{P}}_{k+1} = \mathbf{P}_k / \lambda \quad (9)$$

and

$$\mathbf{K}_{k+1} = \hat{\mathbf{P}}_{k+1} \mathbf{H}_{k+1}^T (\mathbf{H}_{k+1}^T \hat{\mathbf{P}}_{k+1} \mathbf{H}_{k+1} + \lambda)^{-1} \quad (10)$$

respectively, Eqs. (7)–(10) represent the algorithm of RLS method with λ as the forgetting factor and $\lambda \in [0.9, 1.0]$.

If Eq. (6) is rewritten as

$$\mathbf{K}_{k+1} = \mu \mathbf{H}_{k+1}, \quad (11)$$

Eqs. (7) and (11) show the algorithm of LMS method with μ as gradient factor and $\mu \in [0, 1]$.

It's to be noticed that the covariance of process noise, \mathbf{Q}_k , indicates the nonlinearity of the state-space model to some extent i.e., the larger it is the more nonlinearity the model shows. Moreover it has significant influence on the time resolution (effective length of time window) of the model and the covariance of time varying spectrum. In [30–32], a method for choosing \mathbf{Q}_k was set forth. In this study, we find the value of $10^{-4} \mathbf{I}$ (\mathbf{I} is unit matrix) for \mathbf{Q}_k is optimal for most cases.

To initiate the Kalman filter, p initial values of y_k and q zeros are used to construct the measurement vector \mathbf{H}_0 , the state vector \mathbf{X}_0 is estimated based on the corresponding time invariant ARMA model by placing a moving window centered at the initial time of y_k , and \mathbf{P}_0 can be chosen as a large positive definite matrix (e.g., $10^4 \mathbf{I}$). Then, all the state vectors can be estimated step by step. After each iteration, the measurement noise e_k in \mathbf{H}_{k+1} is substituted by the residue \hat{e}_k and σ_k^2 is estimated using $\sigma_k^2 = [(k-1) \cdot \sigma_{k-1}^2 + e_k^2] / k$. The iteration is stopped when the difference between the successive estimation results of σ_k^2 is smaller than a preset limit.

4.2. Estimation of state-space model using unscented Kalman filter

Unscented Kalman filter uses the unscented transformation of a minimal set of deterministic sampling points (Sigma points) to capture the mean and covariance of states, the algorithm is specified as follows:

$$\mathbf{X}_{k+1} = [\mathbf{X}_{0,k+1}, \mathbf{X}_{1,k+1}, \mathbf{X}_{2,k+1}, \dots, \mathbf{X}_{2(p+q),k+1}], \quad (12)$$

$$\hat{\mathbf{X}}_{k+1}^- = \sum_{i=0}^{2(p+q)} W_i^m \mathbf{X}_{i,k+1}, \quad (13)$$

$$\hat{\mathbf{P}}_{k+1} = \sum_{i=0}^{2(p+q)} W_i^c [\boldsymbol{\chi}_{i,k+1} - \hat{\mathbf{X}}_{k+1}^-][\boldsymbol{\chi}_{i,k+1} - \hat{\mathbf{X}}_{k+1}^-]^T + \mathbf{Q}_{k+1}, \quad (14)$$

$$\mathbf{Y}_{k+1} = \mathbf{H}_{k+1}^T \boldsymbol{\chi}_{k+1}, \quad (15)$$

$$\hat{\mathbf{y}}_{k+1}^- = \sum_{i=0}^{2(p+q)} W_i^m \mathbf{Y}_{i,k+1}, \quad (16)$$

$$\mathbf{P}_{\hat{\mathbf{y}}_{k+1}\hat{\mathbf{y}}_{k+1}} = \sum_{i=0}^{2(p+q)} W_i^c [\mathbf{Y}_{i,k+1} - \hat{\mathbf{y}}_{k+1}^-][\mathbf{Y}_{i,k+1} - \hat{\mathbf{y}}_{k+1}^-]^T + \sigma_{k+1}^2, \quad (17)$$

$$\mathbf{P}_{\mathbf{x}_{k+1}\hat{\mathbf{y}}_{k+1}} = \sum_{i=0}^{2(p+q)} W_i^c [\boldsymbol{\chi}_{i,k+1} - \hat{\mathbf{X}}_{k+1}^-][\mathbf{Y}_{i,k+1} - \hat{\mathbf{y}}_{k+1}^-]^T, \quad (18)$$

$$\mathbf{K}_{k+1} = \mathbf{P}_{\mathbf{x}_{k+1}\hat{\mathbf{y}}_{k+1}} \mathbf{P}_{\hat{\mathbf{y}}_{k+1}\hat{\mathbf{y}}_{k+1}}^{-1}, \quad (19)$$

$$\mathbf{X}_{k+1} = \hat{\mathbf{X}}_{k+1}^- + \mathbf{K}_{k+1}(\mathbf{y}_{k+1} - \hat{\mathbf{y}}_{k+1}^-), \quad (20)$$

$$\mathbf{P}_{k+1} = \hat{\mathbf{P}}_{k+1} - \mathbf{K}_{k+1} \mathbf{P}_{\hat{\mathbf{y}}_{k+1}\hat{\mathbf{y}}_{k+1}} \mathbf{K}_{k+1}^T, \quad (21)$$

where $\boldsymbol{\chi}_{k+1}$ are deterministic sampling points (sigma points) given by

$$\begin{cases} \boldsymbol{\chi}_{0,k+1} = \mathbf{X}_k \\ \boldsymbol{\chi}_{i,k+1} = \mathbf{X}_k + (\sqrt{(p+q+\lambda)\mathbf{P}_k})_i & i \in [1, p+q] \\ \boldsymbol{\chi}_{i,k+1} = \mathbf{X}_k - (\sqrt{(p+q+\lambda)\mathbf{P}_k})_i & i \in [p+q+1, 2(p+q)] \end{cases}, \quad (22)$$

and $(\sqrt{(p+q+\lambda)\mathbf{P}_k})_i$ is the i th column (row) of the square root of matrix $(p+q+\lambda)\mathbf{P}_k$ with $\lambda = \alpha^2/(p+q+\kappa)$. The constant α determines the spread of the Sigma points around \mathbf{X}_k and is usually assigned to a small positive value (e.g., $10^{-4} \leq \alpha \leq 10^{-1}$). The constant κ is a secondary parameter which is related to the kurtosis of $\boldsymbol{\chi}_{k+1}$ and is usually set to 0 or $3-p-q$. The weights W_i^c and W_i^m are given by

$$\begin{cases} W_0^m = \lambda/(p+q+\lambda) \\ W_0^c = \lambda/(p+q+\lambda) + (1-\alpha^2+\beta) \\ W_i^m = W_i^c = \lambda/\{2(p+q+\lambda)\} & i \in [1, 2(p+q)] \end{cases}, \quad (23)$$

where β is a constant which is used to incorporate prior knowledge of the distribution of state vector and for Gaussian distribution it can be set to 2 optimally. Eq. (12) shows the process of deterministic sampling and Eqs. (13)–(21) show the process of state estimation by unscented transformation of sigma points [15,18–21].

With the same initial conditions and stopping criterion as that for Kalman filter, the unscented Kalman filter is implemented step by step to estimate the state.

4.3. Difference between Kalman filter and unscented Kalman filter

It can be seen that both the Kalman filter and the unscented Kalman filter consist of the recursion of prediction–updating–estimation. For the Kalman filter the explicit equations of the prediction and covariance of the states and the gain can be derived simply with the assumptions of Gaussian noise and linear model, while in the unscented Kalman filter such quantities are estimated by unscented transformation. Only in cases of Gaussian noise and linear model the Kalman filter is optimal method in the sense of minimum mean square error. In cases of non-Gaussian noise and nonlinear model, the Gaussian approximation of the non-Gaussian noise and the linearization (first order Taylor series expansion) of the nonlinear model will lead to suboptimal performance and sometimes divergence of the Kalman filter and can only capture the posterior mean and covariance accurately to the first order. On the contrary, the unscented Kalman filter addresses above problems by using unscented transformation with no explicit Jacobian or Hessian calculations and can capture the posterior mean and covariance accurately to the 2nd order [15,18].

4.4. Validation of estimation results

The estimation results for different methods can be validated by checking if the normalized residues are Gaussian distribution at certain level of confidence. The process is summarized as follows [11,26]:

- (1) Normalize the residues as $w_k = \hat{e}_k / \sigma_k$ for $k = 1, 2, \dots, n$ where n is total number of residues.
- (2) Calculate the autocorrelation coefficients of the normalized residues given by $\hat{\rho}_k = \hat{R}_k / \hat{R}_0$ where $\hat{R}_k = \frac{1}{n} \sum_{i=1}^{n-k} (w_i - \bar{w})(w_{i+k} - \bar{w})$ and $\bar{w} = \frac{1}{n} \sum_{i=1}^n w_k$.
- (3) Determine the probability that the autocorrelation coefficients $\hat{\rho}_k$ are located in the range $(-2\sqrt{1/n}, +2\sqrt{1/n})$ at 95% of confidence. According to the asymptotic theory, if w_k are mutual independent $\hat{\rho}_k$ should be Gaussian distribution with the mean and covariance being 0 and $1/n$, respectively, i.e., $\hat{\rho}_k \sim N(0, 1/n)$.

In addition, using the estimates of the time varying ARMA coefficients a set of earthquake ground motions can be synthesized by changing the random number seeds, and the agreement between them and the actual ground motion, regarding the properties in amplitude, frequency, duration and structural dynamic response, can be used to evaluate estimation results for different methods and models. In this study, the acceleration response spectra of the actual and the synthesized ground motions are compared for this purpose.

5. Results and discussions

To demonstrate the performance of the UKF based method and its capability in damage detection, two examples are given here. In the first example, the North–South acceleration component of the 1940 Imperial Valley earthquake recorded at El Centro, California, USA, is analyzed using the KF and UKF based methods in parallel with their nonparametric counterparts, short-time Fourier transform and continuous wavelet transform. The time varying spectra, instantaneous frequencies, normalized residues, acceleration response spectra of the synthesized ground motions are compared and discussed. In the second example, we attempt to use the UKF based method as a tool for structural damage detection. The acceleration components of a 7-story reinforced concrete building, the Van Nuys hotel, during the 1994 Northridge earthquake are used for this purpose. The time varying spectra, instantaneous frequencies and their distribution are examined. In both examples, the Morlet wavelet is applied for continuous wavelet transform and a Hanning window of length 128 points is used for short-time Fourier transform.

5.1. Analysis of the acceleration record El Centro (1940, N–S)

The 1500 sampling points for the first 30 s of the record El Centro (1940, N–S), with $\Delta t = 0.02$ s, are used in this example and the accelerogram is shown in Fig. 1. The AIC criterion is used to select the optimal ARMA model order. To make the ARMA model more physically meaningful, the orders in the form of $(2n, 2n - 1)$ are used on purpose, for it has been pointed out in [33,34] that an ARMA $(2n, 2n - 1)$ model is equivalent to

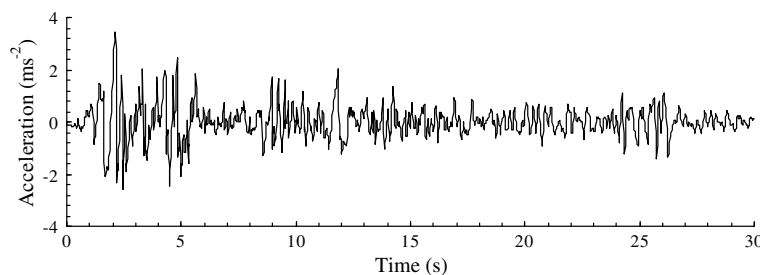


Fig. 1. Accelerogram of the record El Centro (1940, N–S).

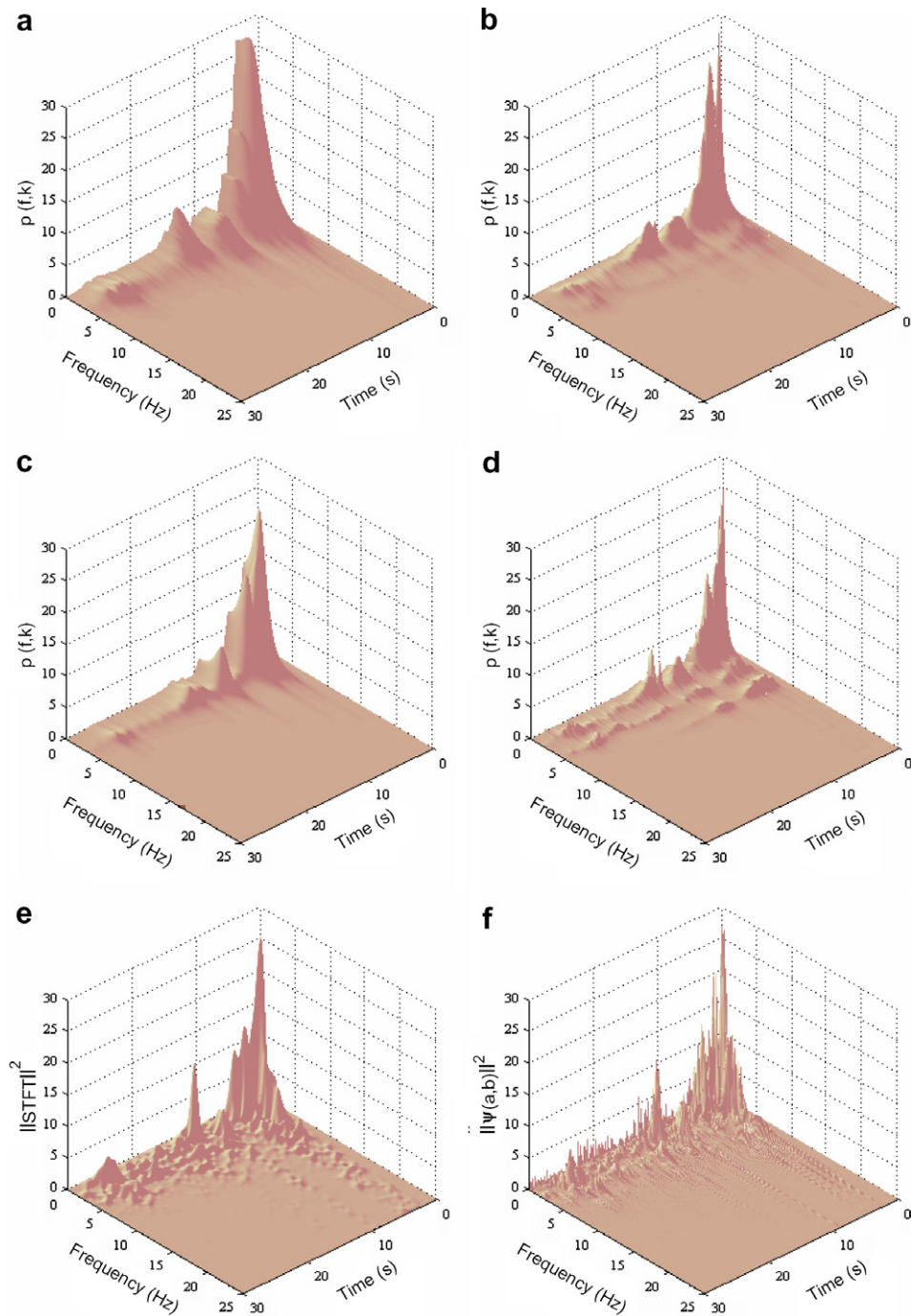


Fig. 2. Time varying spectra corresponding to various ARMA models and estimation methods: (a) ARMA (2, 1)-KF; (b) ARMA (8, 7)-KF; (c) ARMA (2, 1)-UKF; (d) ARMA (8, 7)-UKF; (e) STFT; (f) WT.

an n degrees-of-freedom system. The optimal order is found to be (8, 7) according to the AIC criterion and the corresponding effective frequency range is 0.417–24.167 Hz. To demonstrate the effect of the ARMA model order on estimation results, the ARMA (2, 1) model is also used and its effective frequency range is 2.083–20.833 Hz.

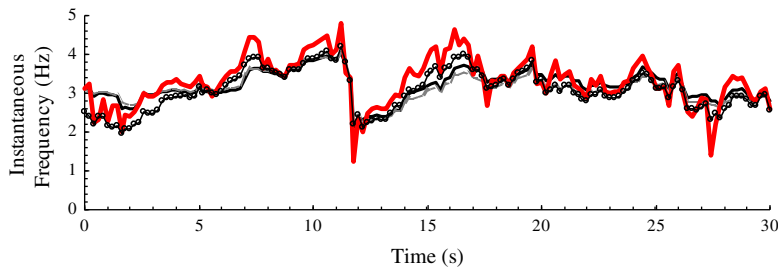


Fig. 3. Comparison of instantaneous frequencies for parametric methods: ARMA (2, 1)-KF; —○— ARMA (2, 1)-UKF; — ARMA (8, 7)-KF; — ARMA (8, 7)-UKF.

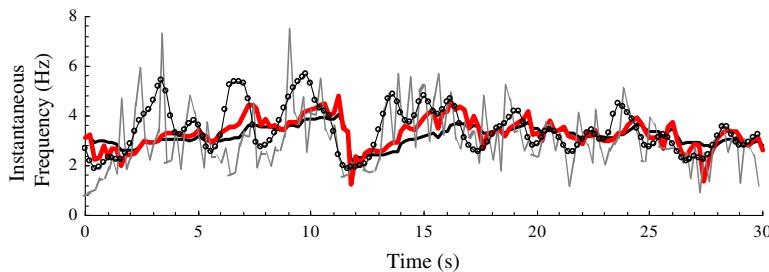


Fig. 4. Comparison of instantaneous frequencies for parametric and nonparametric methods: — ARMA (8, 7)-KF; — ARMA (8, 7)-UKF; —○— STFT; WT.

5.1.1. Comparison of the time varying spectra

The time varying spectra estimated using the KF and UKF based methods with the model orders as (2, 1) and (8, 7) are shown in Figs. 2(a)–(d), and the corresponding results for short-time Fourier transform and continuous wavelet transform are shown in Figs. 2(e) and (f). The results of both parametric and nonparametric methods exhibit the same tendency for energy distribution as a whole, i.e., the majority of the seismic energy is distributed along the horizontal belts below 5 Hz in the first 10 s with several local apexes occurring at about 2, 10, 15 and 25 s. Compared to the results of parametric methods, the results of nonparametric methods are a little blurred and diffused. They represent a much wider frequency band that the seismic energy covers. Along the horizontal belts above 10 Hz in the first 10 s, they overestimate the energy distribution which is mainly because, as has been discussed in [30–32], too short length of effective time window used at higher frequencies may lead to worse frequency resolution and larger spectral variance. The results of parametric methods, on the contrary, are smoother and more legible and represent a narrower frequency band that the seismic energy covers. They provide better readability and more clearly depict the change of frequency content with time.

From the results of different ARMA models, it can be seen that the results of ARMA (8, 7) models provide better time and frequency resolution than those of ARMA (2, 1) models. At frequencies below 2 Hz for the results of ARMA (2, 1) models, there exist obvious blind regions where the spectra are flattened. This is mainly because the effective frequency range for an ARMA (2, 1) model is not wide enough to distinguish the adjacent the spectral peaks.

Comparing the results of KF and UKF based methods, we can see that the results of UKF based methods more clearly distinguish the spectral peaks with improved localization in both time and frequency domains. They also more precisely track the change of frequency content with time.

5.1.2. Comparison of instantaneous frequencies

Here we define the instantaneous frequency as the first order moment of the time varying spectrum with respect to frequency, which physically means the center of gravity of the time varying spectrum in frequency. Figs. 3 and 4 present the instantaneous frequencies calculated according to the time varying spectra in Fig. 2.

Table 1
Probabilities of $\hat{\rho}_k$ in the range $(-1/1500, 1/1500)$

Model and method	Probabilities (%)
ARMA(2,1) and KF	96.61
ARMA(8,7) and KF	97.07
ARMA(2,1) and UKF	98.68
ARMA(8,7) and UKF	99.18

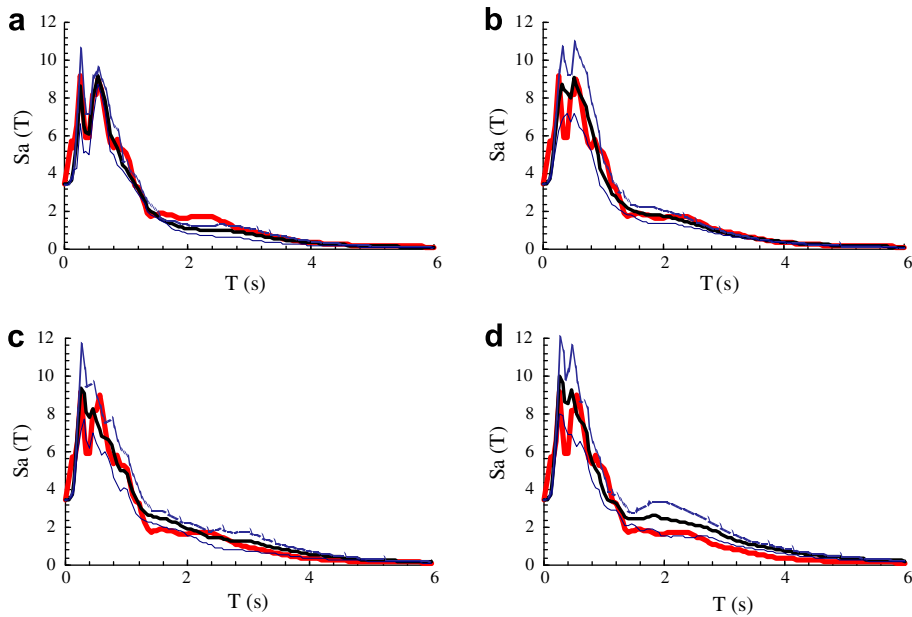


Fig. 5. Comparison of the acceleration response spectra of the synthesized ground motions corresponding to various models and methods: (a) ARMA (8, 7)-UKF; (b) ARMA (8, 7)-KF; (c) ARMA (2, 1)-UKF; (d) ARMA (2, 1)-KF. Key: — El Centro (1940, N-S); — Mean; — Mean plus standard deviation; — Mean minus standard deviation.

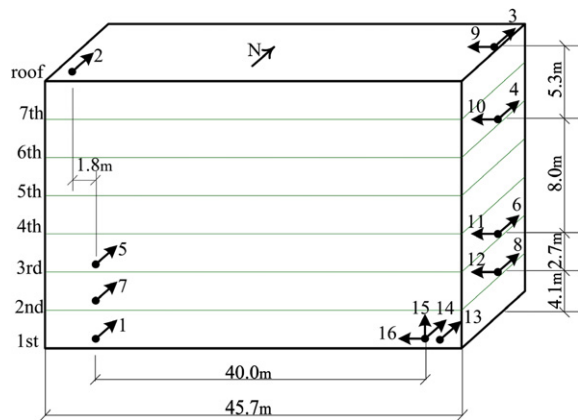


Fig. 6. Sensor locations and orientations of the recording system for the Van Nuys hotel.

As can be seen from Fig. 3, the results of parametric methods show the same tendency and there is very little difference between them. Before 10 s, they increase from 2 to 4 Hz gradually. From 10 to 12 s, they decrease from 4 to 2 Hz drastically. Then, from 12 to 16 s, they increase from 2 to 4 Hz again. And after 16 s, they decrease from 4 to 2.5 Hz slowly.

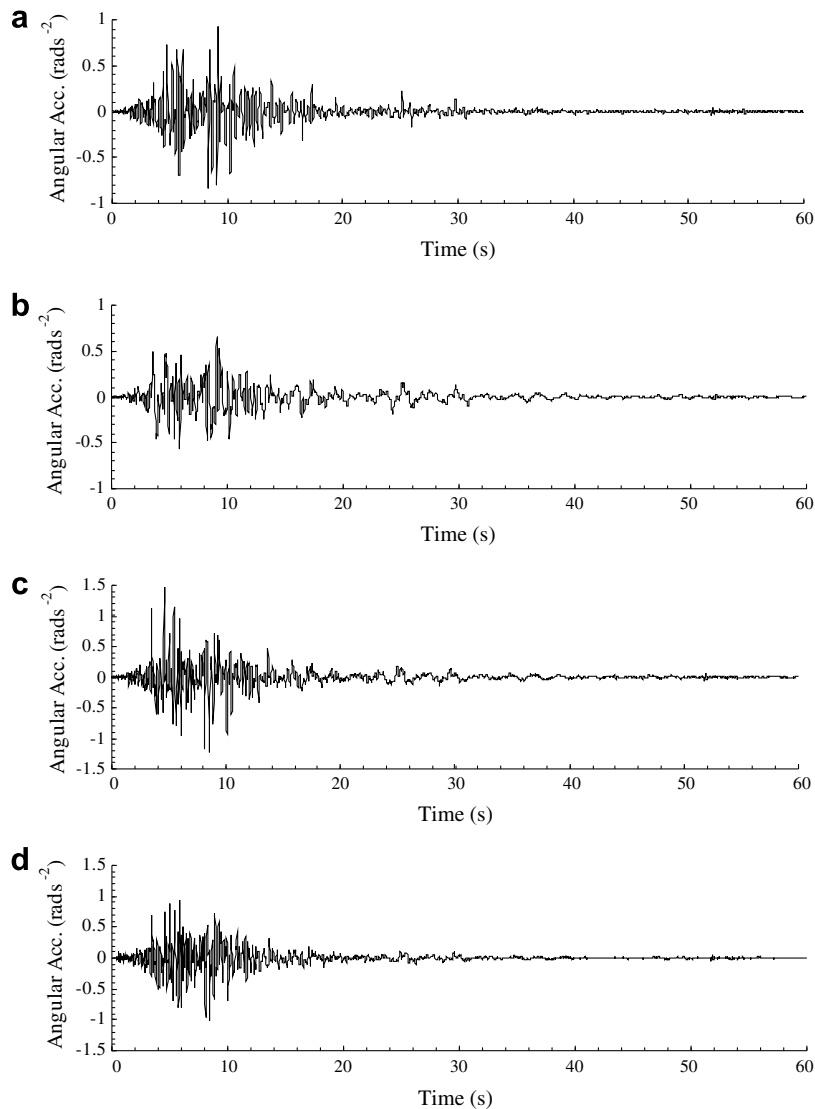


Fig. 7. Relative angular accelerations of the Van Nuys hotel during the 1994 Northridge earthquake: (a) $a_{9,10}$; (b) $a_{10,11}$; (c) $a_{11,12}$; (d) $a_{12,16}$.

From Fig. 4, we can see that the instantaneous frequencies for nonparametric methods have the same general tendency as their parametric counterparts but present much more local fluctuations. Moreover, they are probably overestimated due to the poor frequency resolution at higher frequencies, especially in the first 10 s, as discussed above.

5.1.3. Comparison of residues

Table 1 presents the probabilities that the autocorrelation coefficients of the normalized residues are located in the range $(-1/1500, 1/1500)$. It is clear that ARMA (8, 7) models are better than ARMA (2, 1) models and the UKF based methods outperform the KF based methods.

5.1.4. Comparison of response spectra of the synthesized ground motions

By changing the random number seeds, four sets of ground motions are synthesized according to the time varying ARMA coefficients estimated using the KF and UKF based methods with model orders as (2, 1) and

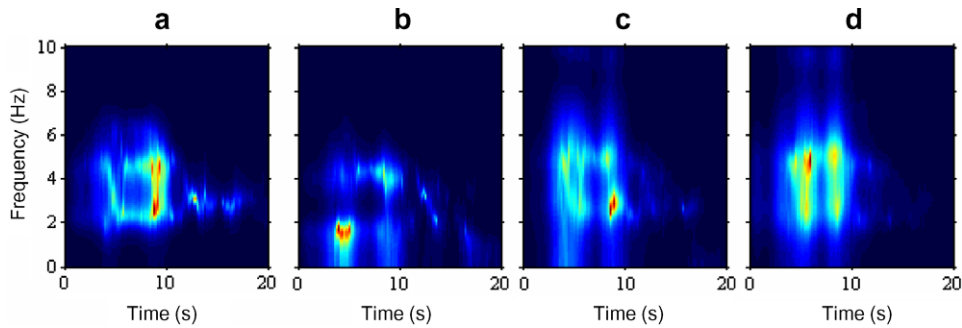


Fig. 8. Time varying spectra estimated using KF based method: (a) $a_{9,10}$; (b) $a_{10,11}$; (c) $a_{11,12}$; (d) $a_{12,16}$.

(8, 7). Each set consists of 100 ground motions. Though there are a lot of quantities available for evaluating the agreement between the synthesized and actual ground motions, the response spectrum is undoubtedly an important one. Fig. 5 shows the acceleration response spectra of the synthesized and actual ground motions with the damping ratio as 5%. The agreement is best in Fig. 5(a), better in Fig. 5(b), and acceptable in Figs. 5(c) and (d). In the short period range below 0.4 s, the agreement in Figs. 5(c) and (d) is worse and in the period range from 1.5 to 3 s, larger discrepancy is shown in Fig. 5(d).

5.2. Damage detection of the Van Nuys hotel

In this example, the UKF based is applied to detect the damage of the Van Nuys hotel caused by the 1994 Northridge earthquake. It was reported that severe shear cracks (width > 5 cm) occurred at the middle columns of the exterior south frame on the 5th floor [35,36] during this earthquake event. The sensor locations and orientations of the recording system for the building are shown in Fig. 6. To eliminate the effect of the nonlinearities in the response of the foundation soil, as discussed in [35], the relative angular accelerations are used to identify the damage of the building. The relative angular acceleration $a_{i,j}$ is given by $a_{i,j} = (a_i - a_j)/d_{i,j}$ where a_i and a_j , respectively, denote the accelerations of the sensors i and j with the distance as $d_{i,j}$. Here, the relative angular accelerations $a_{9,10}$, $a_{10,11}$, $a_{11,12}$ and $a_{12,16}$ are used and the accelerograms are shown in Fig. 7. It is clear that the energy of these relative angular accelerations mainly distributes in the first 20 s. Thus, only the portions for the first 20 s are used for analysis. The optimal order for ARMA models is found to be (16, 15) according to the AIC criterion.

The time varying spectra estimated using various methods are shown in Figs. 8–11. We can see that the energy of $a_{10,11}$ mainly distributes in the frequency range below 2 Hz, while for the other three relative angular accelerations the energy mainly distributes in the frequency range above 2 Hz. This difference can indicate that there is damage in the zone between sensors 10 and 11, i.e., between the 4th and 6th floors. Because the plan

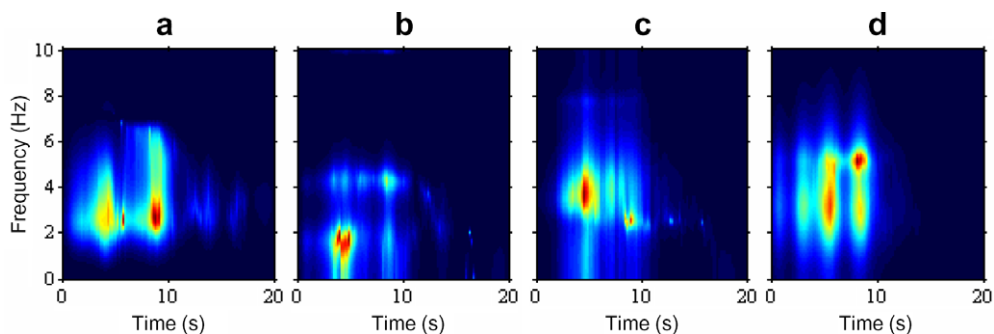


Fig. 9. Time varying spectra estimated using UKF based method: (a) $a_{9,10}$; (b) $a_{10,11}$; (c) $a_{11,12}$; (d) $a_{12,16}$.

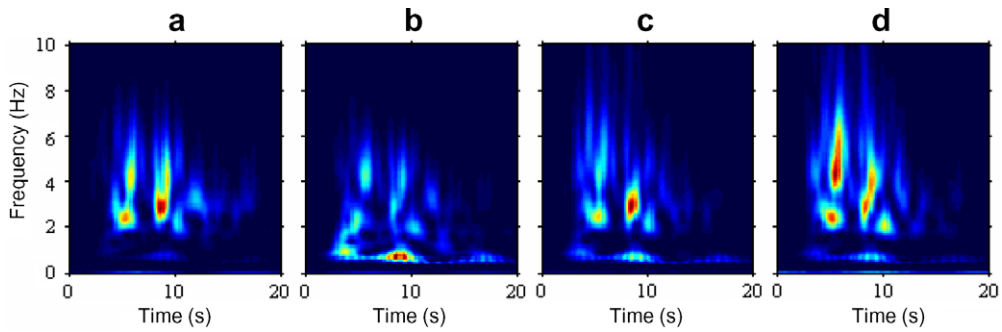


Fig. 10. Time varying spectra estimated using WT: (a) $a_{9,10}$; (b) $a_{10,11}$; (c) $a_{11,12}$; (d) $a_{12,16}$.

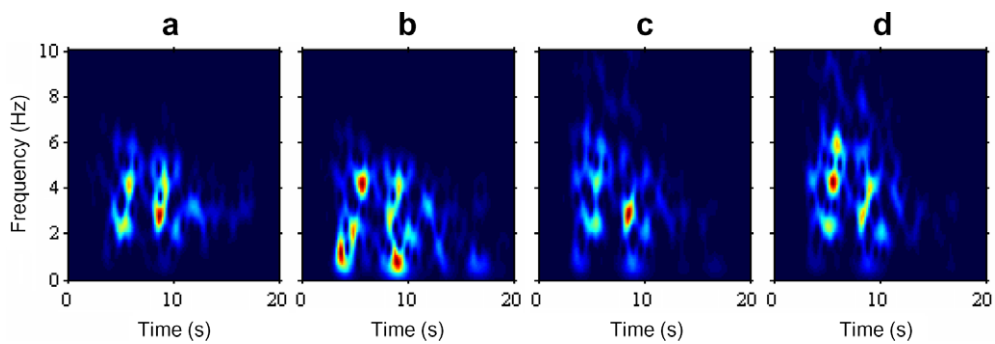


Fig. 11. Time varying spectra estimated using STFT: (a) $a_{9,10}$; (b) $a_{10,11}$; (c) $a_{11,12}$; (d) $a_{12,16}$.

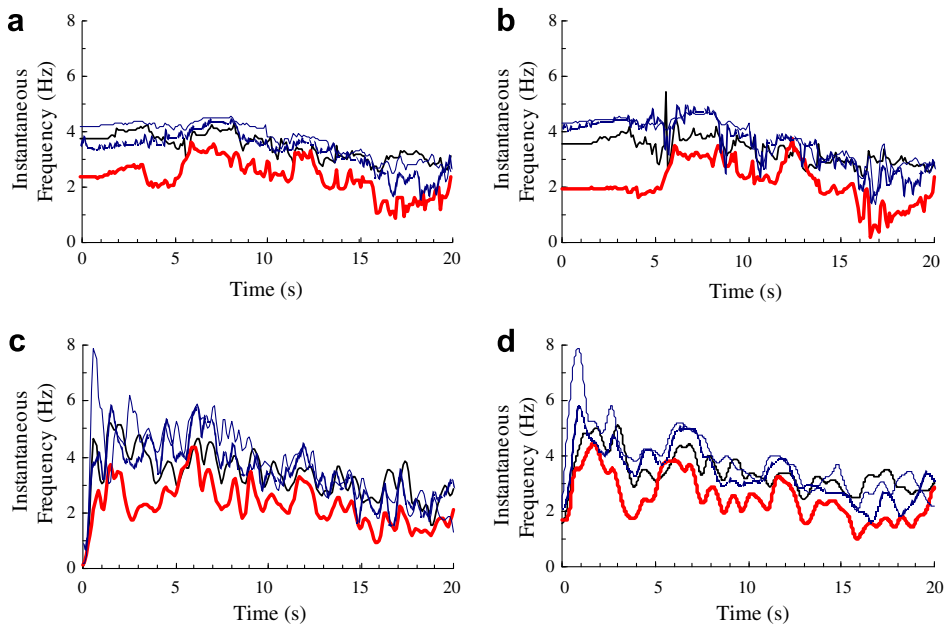


Fig. 12. Instantaneous frequencies corresponding to the time varying spectra in Figs 9–12: (a) KF based method; (b) UKF based method; (c) WT; (d) STFT. Key: $a_{9,10}$ (black solid line); $a_{10,11}$ (red solid line); $a_{11,12}$ (blue dotted line); $a_{12,16}$ (blue solid line).

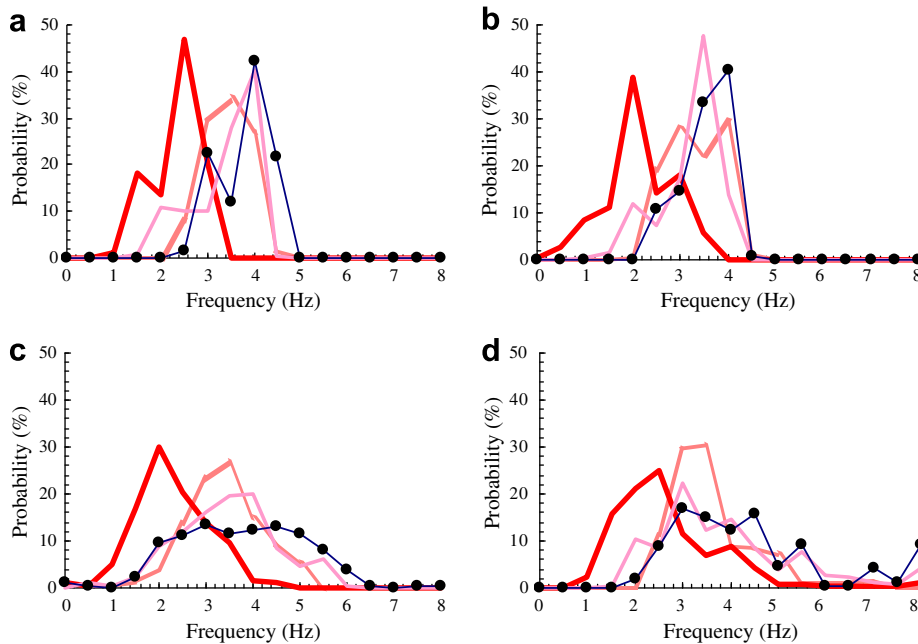



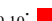


Fig. 13. Statistical distribution of the instantaneous frequencies in Fig. 13: (a) KF based method; (b) UKF based method; (c) WT; (d) STFT. Key:  $a_{9,10}$;  $a_{10,11}$;  $a_{11,12}$;  $a_{12,16}$.

configurations of all the floors of the building are the same, the difference should be mainly caused by the decrease of stiffness due to the damage of the buildings. It can also be seen that this difference is much clearer in Figs. 8 and 9 than in Figs. 10 and 11 where this difference is somewhat blurred because of poor frequency resolution at higher frequencies for nonparametric methods. Furthermore, by comparing Figs. 8 and 9 we can see that the localization of energy and tracking ability in Fig. 9 are a little better and the spectral peaks are more distinctive.

The instantaneous frequencies corresponding to the time varying spectra in Figs. 8–11 are illustrated in Fig. 12. From them, we can see that the instantaneous frequency of $a_{10,11}$ is smaller than the other three for most of the time and there is an obvious decreasing tendency in the instantaneous frequencies after 6 s. But in Figs. 12(c) and (d), the instantaneous frequencies before 5 s are considerably overestimated. There is no noticeable difference between the results presented in Figs. 12(a) and (b), as has been pointed out above, the instantaneous frequencies based on the first order moment of the time varying spectra in frequency are stable to parametric methods.

Fig. 13 demonstrates the statistical distribution of the instantaneous frequencies in Fig. 12. It is shown that the instantaneous frequency of $a_{10,11}$ is mainly distributed in the frequency range from 1.5 to 2.5 Hz but for $a_{9,10}$, $a_{11,12}$, and $a_{12,16}$ the instantaneous frequencies are mainly distributed in the frequency range from 3 to 4.5 Hz. This difference is clearly presented in Figs. 13(a) and (b) and slightly illegible in Figs. 13(c) and (d) due to the overestimation of the instantaneous frequencies. Thus we can see from Figs. 13(c) and (d) that for $a_{9,10}$, $a_{11,12}$, and $a_{12,16}$ more instantaneous frequencies are distributed in the frequency range above 5 Hz.

6. Conclusions

In this study, an UKF based method using time varying ARMA model was proposed to estimate the time varying spectra of earthquake ground motions. Compared with the KF based method and its nonparametric counterparts, the UKF based method offered advantages such as improved accuracy, resolution and tracking, which ensured its better ability to study the local properties of earthquake ground motions and to identify the systems with nonlinearity. We also demonstrated that the effective frequency ranges for ARMA models which

were usually neglected in former studies had considerable effect on the time varying spectra and it should be one of the key factors for order selection of ARMA models. The analysis of the seismic response of the Van Nuys hotel during the 1994 Northridge earthquake showed that the UKF based method was a powerful tool for structural damage detection. The applications of the UKF based method in modeling and attenuation laws determination of time varying spectrum, synthesis of ground motions and dynamic feature extraction for vibration based damage detection were expected as the promising areas for future research.

Acknowledgement

This work was supported by National Natural Science Foundation of China under Grant Nos. 50008017 and 50578167.

References

- [1] I.D. Gupta, M.D. Trifunac, A note on the nonstationarity of seismic response of structures, *Eng. Struct.* 22 (2000) 1567–1577.
- [2] L. Cohen, Time–frequency distributions: a review, *Proc. IEEE* 77 (1989) 941–981, doi:10.1109/5.30749.
- [3] L. Cohen, *Time–frequency Analysis*, PTR Prentice–Hall, 1995.
- [4] H.L. Nikias, A.P. Petropulu, *Higher-Order Spectral Analysis*, PTR Prentice–Hall, 1993.
- [5] M.B. Priestley, Evolutionary spectra and non-stationary processes, *J. Royal Stat. Soc. B27* (1965) 204–237.
- [6] A. Grossmann, J. Morlet, Decomposition of hardy functions into square integrable wavelets of constant shape, *SIAM J. Math. Anal.* 15 (1984) 723–736, doi:10.1137/0515056.
- [7] S. Mallat, *A Wavelet Tour of Signal Processing*, second ed., Academic Press, 1999.
- [8] N.E. Huang, Z. Shen, S.R. Long, M.C. Wu, H.H. Shih, Q. Zheng, N.C. Yen, C.C. Tung, H.H. Liu, The empirical mode decomposition and the Hilbert spectrum for nonlinear and non-stationary time series analysis, *Proc. Royal Soc. Lond. A* 454 (1998) 903–995.
- [9] A.G. Poulimenos, S.D. Fassois, Parametric time-domain methods for non-stationary random vibration modelling and analysis: A critical survey and comparison, *Mech. Syst. Signal Process.* 20 (2006) 763–816.
- [10] Y. Grenier, Time-dependent ARMA modeling of nonstationary signals, *IEEE Trans. Acoust. Speech Signal Process.* 31 (1983) 899–911.
- [11] J.P. Conte, P.S. Pister, S.A. Mahin, Influence of the earthquake ground motion process and structural properties on response characteristics of simple structures, *Earthquake Engineering Research Center UCB/EERC-90/09*, 1990.
- [12] R.E. Kalman, A new approach to linear filtering and prediction problems, *ASME J. Basic Eng.* 82 (1960) 35–45.
- [13] H.W. Sorenson, Least-square estimation: from Gauss to Kalman, *IEEE Spec.* 7 (1970) 63–68.
- [14] L. Ljung, *System Identification: Theory for the User*, second ed., Prentice–Hall, 1999.
- [15] S. Haykin, *Kalman filtering and neural networks*, John Wiley, 2001.
- [16] M.S. Grewal, P.A. Andrews, *Kalman filtering: theory and practice using Matlab*, second ed., John Wiley, 2001.
- [17] M.S. Arulampalam, S. Maskell, N. Gordon, T. Clapp, A tutorial on particle filters for online nonlinear non-Gaussian Bayesian tracking, *IEEE Trans. Signal Process.* 50 (2002) 174–188.
- [18] S. Julier, J.K. Uhlmann, A new extension of the Kalman filter to nonlinear system, in: *Proceedings of the 11th International Symposium on Aerospace/Defence Sensing, Simulation and Controls*, Orlando, Florida, 1997.
- [19] R. Merwe, E.A. Wan, Efficient derivative-free Kalman filters for online learning, in: *Proceedings of European Symposium on Artificial Neural Networks*, Bruges, Belgium, 2001.
- [20] E.A. Wan, R. Merwe, The unscented Kalman filter for nonlinear estimation, in: *Proceedings of IEEE Adaptive Systems for Signal Processing, Communications, and Control Symposium*, Lake Louise, Canada, 2000, pp. 153–158.
- [21] C. Andrieu, A. Doucet, Recursive Monte Carlo algorithms for parameter estimation in general state models, in: *Proceedings of the 11th IEEE Signal Processing Workshop on Statistical Signal Processing*, Singapore, 2001, pp. 14–17.
- [22] P.D. Spanos, M.P. Mignolet, ARMA Monte Carlo simulation in probabilistic structural analysis, *Shock Vibr. Digest* 21 (1989) 3–14.
- [23] M. Shinozuka, E. Samaras, A. Tsurui, ARMA representation of random processes, *ASCE J. Eng. Mech.* 111 (1985) 449–461.
- [24] F. Kozin, ARMA models of earthquake records, *Probab. Eng. Mech.* 3 (1988) 58–63.
- [25] H. Akaike, A new look at the statistical model identification, *IEEE Trans. Autom. Contr.* 19 (1974) 716–723.
- [26] H. Akaike, Use of statistical models for time series analysis, in: *Proceedings of IEEE ICASSP86*, Tokyo, 1986, pp. 3147–3155.
- [27] P.M.T. Broersen, Auto spectral analysis with time series models, *IEEE Trans. Instrum. Measure.* 51 (2002) 3550–3558.
- [28] Y.H. Kang, L.S. He, S.Z. Yang, The theoretical frequency resolving power of ARMA spectrum, *J. Huazhong Univ. Sci. Technol.* 23 (1995) 101–104 (in Chinese).
- [29] P. Jong, J. Penzer, The ARMA model in state space form, *J. Stat. Probab. Lett.* 70 (2004) 119–125.
- [30] F. Gustafsson, S. Gunnarsson, L. Ljung, Shaping frequency-dependent time resolution when estimation spectral properties with parametric methods, *IEEE Trans. Signal Process.* 45 (1997) 160–163.
- [31] S. Gunnarsson, L. Ljung, Frequency domain tracking characteristics of adaptive algorithms, *IEEE Trans. Acoust. Speech Signal Process.* 37 (1989) 1072–1089.

- [32] L. Guo, L. Ljung, Performance analysis of general tracking algorithms, *IEEE Trans. Autom. Contr.* 40 (1995) 1388–1402.
- [33] P. Andersen, Identification of Civil Engineering Structures Using ARMA Models, PhD Thesis, Aalborg University, 1997.
- [34] S.M. Pandit, *Modal and Spectrum Analysis: Data Dependent Systems in State Space*, John Wiley, 1991.
- [35] M.I. Todorovska, S.S. Ivanovic, M.D. Trifunac, Wave propagation in a seven-story reinforced concrete building I. theoretical models, *Soil Dynam. Earthquake Eng.* 21 (2001) 211–223.
- [36] M.D. Trifunac, S.S. Ivanovic, M.I. Todorovska, Instrumented 7-storey reinforced concrete building in Van Nuys, California: description of damage from the 1994 Northridge earthquake and strong motion data, USC Report CE 99-02, 1999.